| | |
|---|---|
| Title | Large magnetocaloric effect and refrigerant capacity in Gd–Co–Ni metallic glasses |
| Author(s) | Zhong, X. C.; Tang, P. F.; Liu, Z. W.; Zeng, D. C.; Zheng, Z. G.; Yu, Hongyu; Qiu, W. Q.; Zhang, Hua; Ramanujan, Raju V. |
| Citation | Zhong, X. C., Tang, P. F., Liu, Z. W., Zeng, D. C., Zheng, Z. G., Yu, H., et al. (2012). Large magnetocaloric effect and refrigerant capacity in Gd–Co–Ni metallic glasses. Journal of Applied Physics, 111(7), 07A919-. |
| Date | 2012 |
| URL | http://hdl.handle.net/10220/9216 |
| Rights |  |

AIP | Journal of Applied Physics

# Large magnetocaloric effect and refrigerant capacity in Gd–Co–Ni metallic glasses

X. C. Zhong, P. F. Tang, Z. W. Liu, D. C. Zeng, Z. G. Zheng et al.

Citation: J. Appl. Phys. **111**, 07A919 (2012); doi: 10.1063/1.3673422
View online: http://dx.doi.org/10.1063/1.3673422
View Table of Contents: http://jap.aip.org/resource/1/JAPIAU/v111/i7
Published by the American Institute of Physics.

# Large magnetocaloric effect and refrigerant capacity in Gd–Co–Ni metallic glasses

X. C. Zhong,[1,a)] P. F. Tang,[1] Z. W. Liu,[1] D. C. Zeng,[1] Z. G. Zheng,[1] H. Y. Yu,[1] W. Q. Qiu,[1] H. Zhang,[2] and R. V. Ramanujan[3]
[1]*School of Materials Science and Engineering, South China University of Technology, Guangzhou 510640, China*
[2]*State Key Laboratory for Magnetism, Institute of Physics, Chinese Academy of Sciences, Beijing 100190, China*
[3]*School of Materials Science and Engineering, Nanyang Technological University, Singapore 639798, Singapore*

(Presented 31 October 2011; received 17 September 2011; accepted 28 October 2011; published online 27 February 2012)

The thermal stability, magnetocaloric effect, and refrigerant capacity (RC) of Gd–Co–Ni metallic glasses were investigated. These alloys possess high glass transition temperature and crystallization temperature as well as a relatively wide supercooled liquid region $\Delta T_x(\Delta T_x = T_x - T_g)$ (40–55 K). With increasing the Co/Ni ratio, the Curie temperature $T_C$ of the amorphous Gd–Co–Ni increases from 140 K to 192 K. For a magnetic field change of 0–5 T, the maximum magnetic entropy change $(-\Delta S_M{}^{max})$ and RC values are in the range of 6.04–6.47 J kg$^{-1}$ K$^{-1}$ and 450–502 J kg$^{-1}$, respectively. These values are comparable with that of $La(Fe_{0.88}Si_{0.12})_{13}$ and higher than those for the well known magnetic refrigerant $Gd_5Si_2Ge_{1.9}Fe_{0.1}$ alloy. The large magnetic entropy change and refrigerant capacity as well as high thermal stability make the alloys attractive candidates as magnetic refrigeration materials for service temperatures of 100–230 K. © *2012 American Institute of Physics*. [doi:10.1063/1.3673422]

## I. INTRODUCTION

Magnetic refrigeration, which has the potential to substitute conventional gas compression refrigeration,[1] is based on the magnetocaloric effect (MCE) of magnetic materials. The basic requirement for magnetic refrigeration materials is a large isothermal magnetic entropy change $\Delta S_M$. However, a material with a large $\Delta S_M$ does not necessarily have high refrigeration efficiency. At present, an accepted criterion to evaluate refrigeration efficiency is refrigerant capacity (RC).[2,3] To obtain a large RC, a broad $\Delta S_M$ peak on $\Delta S_M \sim T$ curve is also needed.

Large MCE has been found in many crystalline materials with a first-order magnetic phase transition (FOMT) like Gd–Si–Ge,[4] La–Fe–Si,[5] Mn–As–Sb,[6] and Mn–Fe–P–As.[7] However, large thermal and/or magnetic hysteresis accompanying the FOMT and the narrow magnetic ordering range results in small RC values. In contrast, some materials with second-order magnetic phase transition (SOMT) have a wide range of magnetic ordering transition temperatures. Although their $\Delta S_M$ is low, their RC value is relatively large.[8,9] Magnetic metallic glasses are an example of such materials with second-order magnetic phase transition and very low hysteresis loss. They also possess special advantages such as tailorable ordering temperature, high thermal stability, high electrical resistivity, high corrosion resistance, and good mechanical properties.[10] In addition, the broad temperature range of the magnetic transition from a paramagnetic to magnetically ordered state also results in high refrigerant capacity.[11] The magnitude of the maximum entropy change of rare-earth-based[12–17] metallic glasses is comparable with that of conventional crystalline Gd,[18] indicating their promising future as candidates for magnetic refrigeration. However, the magnetocaloric effect of metallic glasses has not been fully studied. Here we report on the large magnetocaloric effect and refrigerant capacity in Gd–Co–Ni metallic glasses.

## II. EXPERIMENT

Metallic glasses with the nominal compositions (in at. %) of $Gd_{55}Co_{25+x}Ni_{20-x}$ ($x = 0$, 5, and 10) were prepared in inert

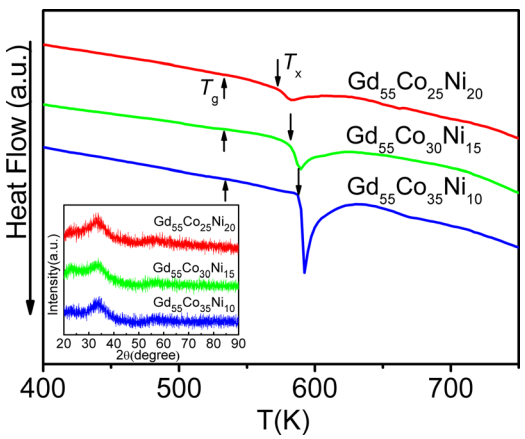


FIG. 1. (Color online) DSC curves of Gd–Co–Ni metallic glasses at a heating rate of 20 K/min. The inset shows the XRD patterns of the Gd–Co–Ni metallic glasses.

a)Author to whom correspondence should be addressed. Electronic mail: xczhong@scut.edu.cn.

 

TABLE I. Thermal parameters of Gd–Co–Ni metallic glasses determined from their DSC traces.

| Materials | $T_g$ (K) | $T_x$ (K) | $\Delta T_x = T_x - T_g$ (K) |
|---|---|---|---|
| $Gd_{55}Co_{25}Ni_{20}$ | 533 | 571 | 38 |
| $Gd_{55}Co_{30}Ni_{15}$ | 533 | 580 | 46 |
| $Gd_{55}Co_{35}Ni_{10}$ | 534 | 589 | 55 |

atmosphere by rapid quenching melt spinning on a single copper wheel with a speed of 50 m/s. X-ray diffraction (XRD) measurements were performed with a Philips diffractometer using Cu $K\alpha_1$ radiation. Differential scanning calorimetry (DSC) data were collected at a heating rate of 20 K/min. The values of glass transition temperature $T_g$ and the onset crystallization temperature $T_x$ were determined from the DSC traces with an accuracy of $\pm 1$ K. Magnetic measurements were carried out by using a Quantum Design Physical Property Measurement System (model PPMS-9).

## III. RESULTS AND DISCUSSION

The XRD patterns of the Gd–Co–Ni metallic glasses are shown in the inset of Fig. 1. Only one broad hump was observed between $2\theta$ of 30° and 35° on each pattern; no well-defined diffraction peaks of crystalline phases are present, indicating that fully amorphous structures are formed. The glassy feature of the specimens is further confirmed by the continuous DSC traces at a heating rate of 20 K/min (Fig. 1). One exothermic peak appeared in the temperature range between 550 and 600 K for all the Gd–Co–Ni metallic glasses, indicating one crystallization transition. With increasing Co/Ni ratio (25:20, 30:15, and 35:10), the crystallization exothermic peak becomes sharper. The values of glass transition temperature ($T_g$) and onset crystallization temperature ($T_x$) as well as the supercooled liquid region $\Delta T_x$ ($\Delta T_x = T_x - T_g$) for Gd–Co–Ni metallic glasses were determined from Fig. 1 and listed in Table I. High $T_g$, $T_x$ and large $\Delta T_x$ were obtained in these alloys, which indicates that these metallic glasses have high thermal stability with respect to crystallization.

The temperature dependence of magnetization for the Gd–Co–Ni metallic glasses measured in an applied field of 0.01 T between 5 and 300 K under zero-field cooling (ZFC) and field cooling (FC) conditions are shown in Fig. 2. The ZFC and the FC curves overlap each other in the whole

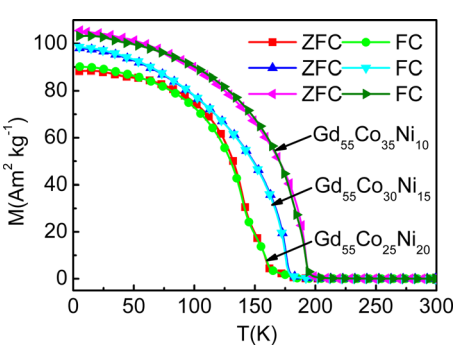


FIG. 2. (Color online) Temperature dependences of magnetization of Gd–Co–Ni metallic glasses measured in a magnetic field of 0.01 T.

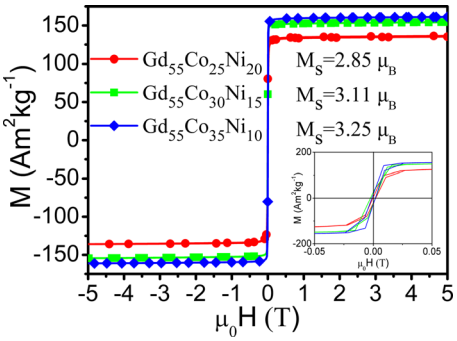


FIG. 3. (Color online) The magnetic hysteresis loops of Gd–Co–Ni metallic glasses measured at 5 K. The inset shows the enlarged part of magnetic hysteresis loops.

temperature range, and no magnetic/thermal hysteresis exists. The Curie temperature ($T_C$) was defined as the temperature at the maximum of $|dM/dT|$-versus-$T$ plot. The Curie temperature $T_C$ was determined to be 140, 175, and 192 K for $Gd_{55}Co_{25+x}Ni_{20-x}$ metallic glasses with $x = 0$, 5, and 10, respectively. With increasing Co/Ni ratio, $T_C$ increases. Figure 3 shows hysteresis loops of Gd–Co–Ni alloys measured at 5 K. All alloys show very good soft magnetic properties with negligible hysteresis and very small coercivity (~20 Oe, shown in the inset of Fig. 3), which is attributed to the very weak magnetic anisotropy as a result of the structural disorder and the zero orbital momentum of Gd atoms. The saturation magnetization ($M_s$) is 136, 154, and 161 Am$^2$ kg$^{-1}$, which corresponds to 2.85, 3.11, and 3.25 $\mu_B$/magnetic atom, for $Gd_{55}Co_{25+x}Ni_{20-x}$ metallic glasses with $x = 0$, 5, and 10, respectively.

Magnetic refrigerants are generally used in the vicinity of their magnetic ordering temperatures. In these metallic glasses, $T_x$ is much higher than the magnetic ordering temperature $T_C$. Hence $Gd_{55}Co_{25+x}Ni_{20-x}$ metallic glasses can be stable in the range of practical application temperatures. Thus, from an engineering point of view, $Gd_{55}Co_{25+x}Ni_{20-x}$ metallic glasses have high temperature stability.

The isothermal magnetization curves for the Gd–Co–Ni metallic glasses were measured with an increasing magnetic field in a wide temperature range. The sweep rate of the field was slow enough to ensure that the data were recorded in an

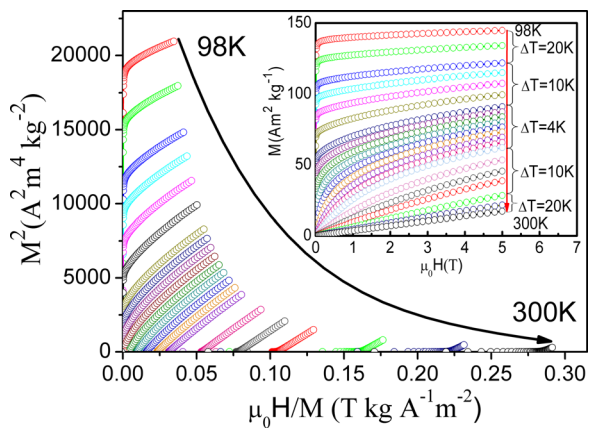


FIG. 4. (Color online) Arrott plots of $Gd_{55}Co_{35}Ni_{10}$ metallic glass constructed from $M(H)$ data. The inset shows the magnetization isotherms of $Gd_{55}Co_{35}Ni_{10}$ metallic glass.

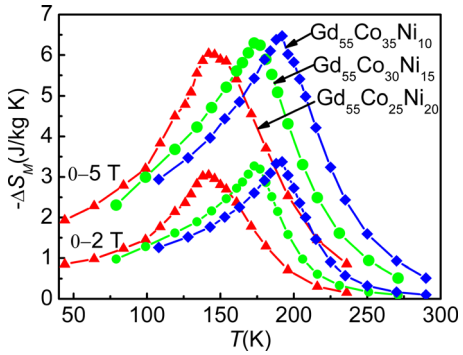


FIG. 5. (Color online) Temperature dependence of magnetic entropy change ($-\Delta S_M$) of Gd–Co–Ni metallic glasses for magnetic field change from 0 to 2 T and 5 T, respectively.

isothermal process. Isothermal magnetization $M(H)$ curves of $Gd_{55}Co_{35}Ni_{10}$ metallic glass are presented in the inset of Fig. 4. A typical ferromagnetic transition is evident in the vicinity of $T_C$. The Arrott plots of $Gd_{55}Co_{35}Ni_{10}$ metallic glass is displayed in Fig. 4. All slopes remain positive, indicating that the ferromagnetic–paramagnetic transition is of second-order.[19]

The MCE of the samples as a function of temperature and magnetic field was calculated from the isothermal magnetization curves using the Maxwell relation. Figure 5 shows the temperature dependences of ($-\Delta S_M$) under different magnetic field changes for the Gd–Co–Ni metallic glasses. The ($-\Delta S_M$) versus $T$ curves display a typical $\lambda$-shape, also indicating that the magnetic phase transition near the Curie temperature of Gd–Co–Ni metallic glasses is a second-order phase transition. For an applied field change from 0 to 5 T, the maximum values of $(-\Delta S_M{}^{max})$ for $Gd_{55}Co_{35}Ni_{10}$, $Gd_{55}Co_{30}Ni_{15}$, and $Gd_{55}Co_{25}Ni_{20}$ metallic glasses are 6.47, 6.30, and 6.04 $Jkg^{-1}K^{-1}$, respectively. These values are much higher than those of $Gd_{55}Co_{20}Fe_5Al_{20}$ (2.24 $Jkg^{-1}K^{-1}$ at 20 kOe) BMG alloy,[20] and $Gd_{65}Fe_{20}Al_{15-x}B_x$ glassy ribbons.[21]

The RC values of these metallic glasses were calculated by numerically integrating the area under the ($-\Delta S_M$) versus $T$ curves, using the temperatures at half maximum of the peak as the integration limits.[3] When the applied field changes from 0 to 5 T, RC values of $Gd_{55}Co_{35}Ni_{10}$, $Gd_{55}Co_{30}Ni_{15}$, and $Gd_{55}Co_{25}Ni_{20}$ are 502, 487, and 450 $Jkg^{-1}$, respectively. These values are comparable to or even much higher than the most well-known crystalline magnetic refrigeration materials, such as $La(Fe_{0.88}Si_{0.12})_{13}$,[22] $Gd_6Co_2Si_3$,[23] $Gd_5Si_2Ge_2$,[9] and $Gd_5Ge_{1.9}Si_2Fe_{0.1}$ (Ref. 9) (Table II). For these Gd–Co–Ni metallic glasses, structural disorder results in exchange integral fluctuations, yielding a wide range of magnetic ordering transition temperatures.[24] Therefore, relatively large RC values are obtained.

TABLE II. Magnetocaloric properties upon applying a field $H$ to various materials and related parameters. (GR and C stand for glassy ribbon and crystalline, respectively.)

| Material | Structure | $T_C$ (K) | $-\Delta S_M$ ($Jkg^{-1}K^{-1}$) | RC ($Jkg^{-1}$) | Applied field ($T$) | Reference |
|---|---|---|---|---|---|---|
| $Gd_{55}Co_{25}Ni_{20}$ | GR | 140 | 6.04 | 450 | 5 | This work |
| $Gd_{55}Co_{30}Ni_{15}$ | GR | 175 | 6.30 | 487 | 5 | This work |
| $Gd_{55}Co_{35}Ni_{10}$ | GR | 192 | 6.47 | 502 | 5 | This work |
| $Gd_5Ge_2Si_2$ | C | 275 | 20.0 | 305 | 5 | 9 |
| $Gd_5Ge_{1.9}Si_2Fe_{0.1}$ | C | 305 | 7.0 | 360 | 5 | 9 |
| $La(Fe_{0.88}Si_{0.12})_{13}$ | C | 195 | 23 | 452 | 5 | 22 |
| $Gd_6Co_2Si_3$ | C | 295 | 6.3 | 503 | 5 | 23 |

## IV. CONCLUSIONS

$Gd_{55}Co_{25+x}Ni_{20-x}$ ($x=0$, 5, and 10) metallic glasses were prepared by the melt-spinning technique. All of these metallic glasses were ordered ferromagnetically and underwent a second-order transition at their Curie temperatures. Negligible coercive force and hysteresis, good thermal stability, and large MCEs and RC of $Gd_{55}Co_{25+x}Ni_{20-x}$ metallic glasses suggest that the alloys are good candidates for active magnetic refrigeration applications in the temperature interval range of 100–230 K.

## ACKNOWLEDGMENTS

This work is financially supported by the Guangdong Provincial Science and Technology Program (Grant Nos. 2010B050300008 and 2009B090300273) and the Fundamental Research Funds for the Central Universities, SCUT (Grant Nos. 2011ZM0014 and 2012ZZ0013).

[1]K. A. Gschneidner, Jr., V. K. Pecharsky, and A. O. Tsokol, Rep. Prog. Phys. **68**, 1479 (2005).
[2]M. E. Wood and W. H. Potter, Cryogenics **25**, 667 (1985).
[3]K. A. Gschneidner, Jr., V. K. Pecharsky, A. O. Pecharsky, and C. B. Zimm, Mater. Sci. Forum **315**, 69 (1999).
[4]V. K. Pecharsky and K. A. Gschneidner, Jr., Phys. Rev. Lett. **78**, 4494 (1997).
[5]F. X. Hu, B. G. Shen, J. R. Sun, Z. H. Cheng, G. H. Rao, and X. X. Zhang, Appl. Phys. Lett. **78**, 3675 (2001).
[6]H. Wada and Y. Tanabe, Appl. Phys. Lett. **79**, 3302 (2001).
[7]O. Tegus, E. Brück, K. H. J. Buschow, and F. R. de Boer, Nature (London) **415**, 150 (2002).
[8]D. H. Wang, S. L. Huang, Z. D. Han, Z. H. Su, W. Q. Zou, and Y. W. Du, J. Alloys Compd. **377**, 72 (2004).
[9]V. Provenzano, A. J. Shapiro, and R. D. Shull, Nature (London) **429**, 853 (2004).
[10]Q. Y. Dong, B. G. Shen, J. Chen, J. Shen, F. Wang, H. W. Zhang, and J. R. Sun, J. Appl. Phys. **105**, 053908 (2009).
[11]A. M. Tishin and Yu. I. Spichkin, *The Magnetocaloric Effect and Its Applications* (IOP, Bristol, 2003), pp. 330–337.
[12]Q. Luo, D. Q. Zhao, M. X. Pan, and W. H. Wang, Appl. Phys. Lett. **89**, 081914 (2006).
[13]H. Fu, M. S. Guo, H. J. Yu, and X. T. Zu, J. Magn. Magn. Mater. **321**, 3342 (2009).
[14]B. Schwarz, B. Podmilsak, N. Mattern, and J. Eckert, J. Magn. Magn. Mater. **322**, 2298 (2010).
[15]L. Liang, X. Hui, C. M. Zhang, and G. L. Chen, Intermetallics **16**, 198 (2008).
[16]Q. Luo, D. Q. Zhao, M. X. Pan, and W. H. Wang, Appl. Phys. Lett. **90**, 211903 (2007).
[17]L. Liang, X. Hui, Y. Wu, and G. L. Chen, J. Alloys Compd. **463**, 30 (2008).
[18]V. K. Pecharsky and K. A. Gschneidner, J. Magn. Magn. Mater. **200**, 44 (1999).
[19]J. S. Kouvel and M. E. Fisher, Phys. Rev. **136**, A1626 (1964).
[20]C. L. Jo, L. Xia, D. Ding, and Y. D. Dong, J. Alloys Compd. **458**, 18 (2008).
[21]Y. K. Fang, C. H. Lai, C. C. Hsieh, X. G. Zhao, H. W. Chang, W. C. Chang, and W. Li, J. Appl. Phys. **107**, 09A901 (2009).
[22]A. Fujita and K. Fukamichi, J. Alloys Compd. **554**, 404 (2005).
[23]J. Shen, J. F Wu, and J. R. Sun, J. Appl. Phys. **106**, 083902 (2009).
[24]X. Y. Liu, J. A. Barclay, R. B. Gopal, M. Foldeaki, R. Chahine, T. K. Bose, P. J. Schurer, and J. L. LaCombe, J. Appl. Phys. **79**, 1630 (1996).